NASA Technical Memorandum 106089
ICOMP-93-9

The Development of a Mixing Layer Under the Action of Weak Streamwise Vortices

Marvin E. Goldstein
Lewis Research Center
Cleveland, Ohio

and

Joseph Mathew
Institute for Computational Mechanics in Propulsion
Lewis Research Center
Cleveland, Ohio

March 1993

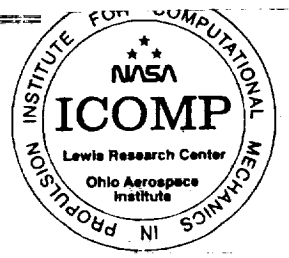

NASA

THE DEVELOPMENT OF A MIXING LAYER UNDER THE ACTION OF WEAK STREAMWISE VORTICES

Marvin E. Goldstein
National Aeronautics and Space Administration
Lewis Research Center
Cleveland, Ohio 44135

Joseph Mathew
Institute for Computational Mechanics in Propulsion
Lewis Research Center
Cleveland, Ohio 44135

The action of weak, streamwise vortices on a plane, incompressible, steady mixing layer is examined in the large-Reynolds-number limit: The outer, inviscid region is bounded by a vortex sheet to which the viscous region is confined. It is shown that the local linear analysis becomes invalid at streamwise distances $O(\epsilon^{-1})$, where $\epsilon \ll 1$ is the crossflow amplitude, and a new nonlinear analysis is constructed for this region. Numerical solutions of the nonlinear problem show that the vortex sheet undergoes an O(1) change in position and that the solution is ultimately terminated by the appearance of a singularity. The corresponding viscous layer shows downstream thickening, but appears to remain well-behaved up to the singular location.

1. Introduction

Mixing layer flows being canonical and of technological importance have been studied extensively over the years. In this paper, some new, three-dimensional and nonlinear features are examined theoretically. We consider a steady, incompressible free shear layer--two nominally uniform streams at different speeds--and study the effect of small nonuniformities imposed on one of these streams. The analysis is restricted to the asymptotically large-

Reynolds-number case for which the usual boundary layer approximation applies: There is an outer, inviscid region with an infinitesimally thin vortex sheet forming the interface between the two streams and an inner, viscous layer that resolves the velocity discontinuity across the vortex sheet. (See figure 1.) We suppose, for definiteness, that the mixing layer forms downstream of an infinitesimally thin splitter plate. The upstream base flow consists of a uniform parallel stream and a second stream at rest in our reference frame. The resulting vortex sheet is then a plane surface in the vicinity of the trailing edge, and the relevant viscous problem admits a similarity solution[1,2] there. (For simplicity, we neglect the upstream boundary layer on the surface of the plate.) We suppose that a small $O(\epsilon)$ streamwise vorticity field is imposed on this flow somewhere upstream of the trailing edge, where $\epsilon \ll 1$ measures crossflow amplitude, and seek a series solution by expanding in powers of ϵ. The $O(\epsilon)$ crossflow is convected without change, and the vortex sheet remains planar to that order. However, the $O(\epsilon^2)$ solution increases linearly with the streamwise coordinate x as x becomes large, so that the series is no longer valid when x is $O(1/\epsilon)$. A new, nonlinear solution therefore has to be found for this region in order to obtain a uniformly valid solution to the problem. A similar situation was found in a study of flat-plate boundary layers subjected to weak nonuniformities in the external stream.[3,4]

As in Goldstein and Leib,[4] the nonlinear flow is governed by the two-dimensional, time-dependent vorticity equation with an appropriately scaled streamwise coordinate playing the role of the time. However, the situation is now considerably more complex because the vortex sheet is displaced by an O(1)

amount in the nonlinear region, and the vorticity equation therefore has to be solved in a region of unknown shape. The problem is also similar to those in Goldstein et al.[3] and Goldstein and Leib,[4] in that the viscous shear flow that bounds the nonlinear region is governed by the three-dimensional boundary layer equations. However, these equations now have to be solved on a curved surface, rather than on a plane surface, and this again makes the problem more complex.

For definiteness, we suppose that the imposed spanwise sinusoidal crossflow has the form of a pair of counter-rotating vortices per period, which then become distorted as the flow evolves downstream. The numerical solution shows that the vortex sheet grows monotonically until the computations break down at (or near) $\epsilon x = 0.8$. The relevant Fourier spectrum suggests that this breakdown is due to the formation of a pair of symmetrically disposed singularities per period.

The breakdown is not completely unexpected, since the vortex sheet boundary condition has the form of an inviscid Burger's equation, with some additional terms arising from the vortex sheet development, and the Burger's equation solutions are known to become singular at finite downstream locations. The present problem also bears some similarity to the (temporally evolving) Kelvin-Helmholtz instability of a disturbed two-dimensional vortex sheet, which is known to produce a finite time singularity.[5] Krasny[6] obtained a numerical solution to this problem and found that when the initial disturbance is sufficiently large, a pair of singularities ultimately form and the attendant Fourier spectrum is similar to the one obtained in the present

case. Krasny[6] used an ad hoc approximation to extend his computations beyond the singular time and found that the vortex sheet rolls up into a pair of tightly wound spirals. We therefore expect that the vortex sheet will also undergo spanwise roll-up in the present case.

The shear layer flow appears to be relatively unaffected by the vortex-sheet distortion. The layer thickness does increase faster than the corresponding Lock profile, but there does not seem to be any dramatic changes as the singularity is approached. This may reflect the fact that the singularity is of higher order, i.e., it only appears in the higher-order derivatives.

2. Formulation

Consider a uniform, parallel, incompressible, steady stream that slips past a semi-infinite but infinitesimally thin flat plate with speed U_∞. A Cartesian coordinate system is centered at the plate's trailing edge, with the x-axis aligned with the main stream and y and z coordinates in the transverse and spanwise directions, respectively. In the large-Reynolds-number limit being considered herein, the undisturbed downstream flow consists of an inviscid parallel flow with a plane vortex sheet in $x > 0$, $y = 0$ and a viscous layer that resolves the resulting velocity discontinuity. Lock[1,2] obtained a similarity solution to the viscous flow. We suppose that a steady crossflow disturbance of $O(\epsilon)(\epsilon << 1)$, with spanwise lengthscale λ, is superposed on this piecewise uniform flow. All quantities are nondimensionalized using appropriate combinations of λ and U_∞. The resulting Reynolds number

$R = \lambda U_\infty/\nu$, where ν is the fluid's kinematic viscosity, is assumed to be sufficiently large ($R >> \epsilon^{-1}$) so that to $O(\epsilon^2)$ the outer flow satisfies the Euler equations:

$$\nabla\cdot\boldsymbol{u}=0 \ ,$$

$$\boldsymbol{u}\cdot\nabla\boldsymbol{u}+\nabla p = 0 \ , \tag{1}$$

where u is the velocity, and p is the pressure. (The $O(R^{-1/2})$ boundary layer displacement effects can be incorporated into u if necessary.) The vortex sheet, located at $y = f(x,z)$, is a material surface and satisfies a kinematic requirement that it move with the fluid velocity, which means that for the steady flow being considered here, the component of velocity normal to the sheet must vanish:

$$\boldsymbol{u}\cdot\nabla(y-f) = 0; \ x>0, y=f(x,z), -\infty<z<\infty. \tag{2}$$

Also, the pressure must be continuous across the sheet in order to ensure that it does not undergo infinite acceleration.

Since the base flow is zero in the region below the sheet, the corresponding induced flow, if it exists, must be irrotational to $O(\epsilon^2)$ and therefore possesses a velocity potential, say Φ^-. However, Φ^- turns out to be a constant, because it is an everywhere bounded solution to Laplace's equation, whose normal derivative vanishes on the (stationary) vortex sheet and plate boundaries. Hence there is no induced flow, the pressure is everywhere constant in $y < f(x,z)$, and the second boundary condition becomes

$$p=0; \ x>0, y=f(x,z), -\infty<z<\infty. \tag{3}$$

The velocities and pressure must remain bounded at large distances from the trailing edge, and the upstream initial conditions require

$$\boldsymbol{u} \to \boldsymbol{u}_0 \ \ as \ \ x \to -\infty, \tag{4}$$

where $u_o(y,z) = (0,v_0,w_0)$ is the imposed crossflow. Continuity of the vortex sheet requires that

$$f = \frac{\partial f}{\partial x} = 0; \; x=0, -\infty < z < \infty \; . \tag{5}$$

2.1. Breakdown of linear solution

Near the trailing edge, the dependent variables expand like

$$u(x,y,z) = (1,0,0) + \epsilon(u_1,v_1,w_1) + \epsilon^2(u_2,v_2,w_2) + \cdots, \tag{6}$$

$$p(w,y,z) = \epsilon p_1 + \epsilon^2 p_2 + \cdots, \tag{7}$$

$$f(x,z) = \epsilon f_1 + \epsilon^2 f_2 + \cdots. \tag{8}$$

Substituting this into equations (1)-(3) and equating powers of ϵ, we find that the $O(\epsilon)$ solution is $f_1 = p_1 = 0$ and

$$\boldsymbol{u}_1 = \{0, v_0, w_0\}, \tag{9}$$

while the $O(\epsilon^2)$ solution satisfies

$$\nabla \cdot \boldsymbol{u}_2 = 0, \tag{10}$$

$$\frac{\partial \boldsymbol{u}_2}{\partial x} + \nabla p_2 = -(\boldsymbol{u}_1 \cdot \nabla)\boldsymbol{u}_1 \tag{11}$$

subject to

$$\begin{aligned} v_2 - \frac{\partial f_2}{\partial x} &= 0; \; x>0, y = 0, -\infty < z < \infty, \\ p_2 &= 0; \; x>0, y = 0, -\infty < z < \infty. \end{aligned} \tag{12}$$

p_2 must remain bounded in the far field, and taking the gradient of equation (11) and using equation (10) shows that p_2 satisfies the Poisson equation

$$\nabla^2 p_2 = -\nabla \cdot [(\boldsymbol{u}_1 \cdot \nabla)\, \boldsymbol{u}_1] \,, \tag{13}$$

while the y-component of equation (11) implies that

$$\frac{\partial p_2}{\partial y} = 0; \; x \le 0, \; y = 0, \; -\infty < z < \infty. \tag{14}$$

Once p_2 is found from these relations, u_2 is a simple quadrature of (10).

It follows that

$$p_2(x, y, z) \sim p_{2\infty}(y, z) \quad (x \to \infty) \,, \tag{15}$$

since both the forcing in equation (13) and the boundary condition (14) become independent of x, as $x \to \infty$. Equations (10) and (11) imply that the corresponding asymptotic behavior of the velocity and sheet displacement are:

$$\boldsymbol{u}_2 \sim -[(\boldsymbol{u}_1 \cdot \nabla)\, \boldsymbol{u}_1 + \nabla p_{2\infty}]\, x \quad (x \to \infty) \,, \tag{16}$$

$$f_2 \sim -\left[(\boldsymbol{u}_1 \cdot \nabla)\, v_1 + \frac{\partial p_{2\infty}}{\partial y} \right] \frac{x^2}{2} \quad (x \to \infty) \,. \tag{17}$$

This shows that $O(\epsilon^2)$ terms become comparable to the $O(\epsilon)$ terms when $\epsilon x \sim O(1)$ and, therefore, that the expansions (6)-(8) are no longer valid in this region.

2.2 Nonlinear inviscid region

To find an appropriate solution for this region (which will turn out to be uniformly valid when $x = O(1)$), we introduce the slow streamwise length scale

$$\overline{x} = \epsilon x \tag{18}$$

and seek an expansion of the form

$$u=1+\epsilon^2\bar{u}(\bar{x},y,z,)+\cdots \quad v=\epsilon\tilde{v}(\bar{x},y,z)+\cdots \quad w=\epsilon\bar{w}(\bar{x},y,z)+\cdots \quad p+\epsilon^2\bar{p}(\bar{x},y,z)+\cdots$$
$$f=\bar{f}(\bar{x},z)+\cdots . \tag{19}$$

Substituting these into equations (1)-(3) and equating powers of ϵ gives

$$\frac{\partial\tilde{v}}{\partial y}+\frac{\partial\bar{w}}{\partial z}=0 \tag{20}$$

$$D\bar{u} = -\frac{\partial\bar{p}}{\partial\bar{x}},\ D\tilde{v} = -\frac{\partial\bar{p}}{\partial y},\ D\bar{w} = -\frac{\partial\bar{p}}{\partial z}, \tag{21}$$

where

$$D \equiv \frac{\partial}{\partial\bar{x}}+\tilde{v}\frac{\partial}{\partial y}+\bar{w}\frac{\partial}{\partial z}, \tag{22}$$

and

$$\tilde{v}-\frac{\partial f}{\partial\bar{x}}-\bar{w}\frac{\partial\bar{f}}{\partial z} = 0;\ \bar{x}>0, y=0, -\infty<z<\infty, \tag{23}$$

$$\bar{p} = 0;\ \bar{x}>0, y=0, -\infty<z<\infty. \tag{24}$$

Matching with the perturbation solution (6) of §2.1 requires that

$$\tilde{v},\bar{w}\to v_0, w_0 \quad as \quad \bar{x}\to 0. \tag{25}$$

Eliminating $\bar{p}$ between equations (21) and (22) yields

$$D\Omega = 0 \tag{26}$$

where

$$\Omega \equiv \frac{\partial\bar{w}}{\partial y}-\frac{\partial\tilde{v}}{\partial z} \tag{27}$$

is the streamwise vorticity. The simple (Prandtl) coordinate transformation

$$\bar{y} = y-\bar{f}(\bar{x},z), \tag{28}$$

transfers the vortex-sheet boundary to the known location $\bar{y} = 0$. The vorticity transport equation (26) remains

$$\bar{D}\Omega = 0 \tag{29}$$

but now with

$$\bar{D} \equiv \frac{\partial}{\partial \bar{x}} + \bar{v}\frac{\partial}{\partial \bar{y}} + \bar{w}\frac{\partial}{\partial z}, \tag{30}$$

where

$$\bar{v} = \tilde{v} - \bar{f}_{\bar{x}} - \bar{w}\bar{f}_z. \tag{31}$$

The kinematic condition (23) is now simply

$$\bar{v} = 0 \ at \ \bar{y} = 0. \tag{32}$$

Equation (20) implies that there exists a crossflow stream function ψ defined by

$$\bar{v} = -\frac{\partial \psi}{\partial z}, \quad \bar{w} = \frac{\partial \psi}{\partial \bar{y}}. \tag{33}$$

Inserting this together with equation (31) into definition (27) shows that

$$\Omega = \psi_{zz} + (1 + \bar{f}_z^2)\,\psi_{\bar{y}\bar{y}} - \psi_{\bar{y}}\bar{f}_{zz} - 2\psi_{\bar{y}z}\bar{f}_z - \bar{f}_{\bar{x}z}. \tag{34}$$

Transforming the second two equations (21) via equations (28) and (31), eliminating $\bar{p}$ from the result, and using conditions (24) and (32), we find that the latter two conditions imply

$$D_0\bar{w} + \bar{f}_z D_0^2 \bar{f} = 0 \ ; \ at \ \bar{y} = 0, \tag{35}$$

where

$$D_0 \equiv \frac{\partial}{\partial \bar{x}} + \bar{w}\frac{\partial}{\partial z}.$$

Thus the problem consists of finding a solution to equations (25), (29), and (33) through (35) that remains bounded at $\bar{y} \to \infty$.

2.3 Viscous layer

The vortex sheet discontinuity is resolved by a thin viscous shear layer of thickness, $\delta = (L/\lambda)O(R_L^{-1/2})$, where R_L is the Reynolds number based on the length L from the origin of the boundary layer, so that $\delta = (\epsilon R)^{-1/2}$ when $\bar{x} = O(1)$. We therefore introduce the scaled transverse coordinate, Y, defined by

$$\bar{y} = \delta Y . \tag{36}$$

Then the streamwise velocity

$$u = U(\bar{x}, Y, z) \tag{37}$$

is O(1), and the requirements of continuity and matching with the outer flow are ensured by the scalings,

$$\epsilon\delta V = v - \epsilon u f_{\bar{x}} - w f_z , \quad w = \epsilon W , \quad p = \epsilon^2 P . \tag{38}$$

Introducing these new scaled variables into the Navier-Stokes equations and retaining only lowest order terms, we find

$$\tilde{D}U = (1 + \bar{f}_z^2)\, U_{YY} , \tag{39}$$

$$(1 + \bar{f}_z^2)\, \tilde{D}W + \bar{f}_z (U\tilde{D}\bar{f}_{\bar{x}} + W\tilde{D}\bar{f}_z) = (1 + \bar{f}_z^2)^2 W_{YY} , \tag{40}$$

$$U_{\bar{x}} + V_Y + W_z = 0 , \tag{41}$$

where

$$\tilde{D} \equiv U\frac{\partial}{\partial \bar{x}} + V\frac{\partial}{\partial Y} + W\frac{\partial}{\partial z} .$$

The boundary conditions are obtained by matching to the outer flow,

$$U \to 1, \quad W \to W_{\infty} \equiv \overline{w}(\overline{x}, \overline{y} = 0, z) \quad (Y \to \infty)$$
$$U \to 0, \quad W \to 0 \quad (Y \to -\infty), \tag{42}$$

Equation (40) becomes identical to (35) when all derivatives with respect to Y are set equal to zero, as required for smooth matching with the outer flow. The initial condition is Lock's[1] solution which is valid for x = O(1), i.e., for $\overline{x} \to 0$.

3. Results

In order to be specific, we consider only the imposed crossflow

$$\overline{v} = coz\ z\ sech\ \overline{y} \tanh \overline{y},$$
$$\overline{w} = -\sin z\ sech\ \overline{y}(2 \tanh^2 \overline{y} - 1),$$
$$\Omega = -6 \sin z\ sech\ \overline{y} \tanh \overline{y}(\tanh^2 \overline{y} - 1).$$

which is initially sinusoidal and decays exponentially as $\overline{y} \to \infty$. Both the inviscid and viscous flow can be computed by marching downstream in $\overline{x}$.

3.1. Inviscid flow

Since the initial crossflow was restricted to spanwise periodic data, Fourier spectral methods can be used in spanwise direction, and we use second-order, finite-difference formulae on uniform grids to compute streamwise and transverse derivatives. The vorticity is obtained at each station $\overline{x}^i$ by the

discretization of equation (29) according to the mid-point, leap-frog method, which is explicit and marginally stable. Next, the stream function $\psi(\bar{x}^i, \bar{y}, z)$ and vortex-sheet displacement $\bar{f}(\bar{x}^i, z)$ are determined sequentially by iteration between equations (34) and (35). All nonlinear terms are evaluated as products in physical space. The computed solutions were tested against a perturbation solution for small $\bar{x}$. The numerical results (presented below) were obtained using $\Delta\bar{x}=0.005, \Delta\bar{y}=0.005$, with the computational region limited to $\bar{y}\leq 5$..

The vortex sheet in the region $0<\bar{x}<0.8, 0<z<2\pi$ is shown in figure 2. Its spanwise form is dominated by the second harmonic of the imposed crossflow. Figures 3 and 4 show the downstream development of sheet displacement $\bar{f}(\bar{x}, z)$ and the spanwise velocity $w(\bar{x}, \bar{y}=0, z)$ at several intermediate stations. The steepening of the velocity profile is reminiscent of the solutions to the inviscid Burger's equation which equation (35) resembles. However, this equation also contains additional terms, due to vortex-sheet displacement which reverses the steepening (about $z = \pi$) near $\bar{x}=0.7$. This can be seen more clearly in figure 5, which is a plot of the derivative, $\partial\bar{w}/\partial z$. Once the steepening reverses, two symmetrically disposed lobes emerge and continue to sharpen until the computations break down. Figure 6 is a contour plot of a crossflow steam function ψ' defined analogously to ψ, but based on the Cartesian variables $\bar{v}, \bar{w}, y, z$. The vortices are attracted towards the $z = \pi$ symmetry plane, and an induced rotation opposite to that in the main flow appears close to the vortex sheet. (Contours end on the vortex sheet because a curved sheet implies a non-zero

velocity in the crossflow plane.) These streamline patterns do not suggest any obvious tendency for singularity formation or breakdown.

The breakdown occurs near $\bar{x}=0.8$. Calculations were repeated with the number of spanwise nodes doubled successively from 32 through 512, corresponding to increasing the highest resolved wavenumber from 16 to 256. In all cases, the breakdown occurs at some $\bar{x}=\bar{x}_s>0.8$ with x_s approaching 0.8 from above, monotonically, as the resolution improves. Moreover, the breakdown occurs on the sheet and not at an interior point.

The route to singularity formation can be observed in the downstream evolution of the spectrum of the solution. Figure 7 is the Fourier spectrum, $\hat{w}_n(x,y=0)$, of the spanwise velocity profiles shown in figure 4. The spectrum must exhibit exponential decay at large wavenumbers as long as the function remains analytic, but energy transfers to higher wavenumbers, and the decay rate decreases as $\bar{x}$ increases. Near $\bar{x} = 0.8$, the exponential decay is eventually lost, and the function is no longer analytic. The nearly periodic oscillations in the high-wave-number component of the spectrum suggest that the singularity initially forms at two spanwise locations, say $z = \pm z_s$ per period. The interval Δn between successive minima in the spectrum is approximately 16, suggesting that $z_s = \pi/16$, which is approximately the distance from the symmetry plane of the two minima in figure 5. The spectrum does not seem to suggest that the oscillatory tail is due to spurious growth at the highest wavenumbers.

3.2. Viscous layer

The viscous layer is driven by the tangential velocity over a distorted vortex sheet. It is computed by an adaption of the Keller-box scheme,[7] which is used to march downstream from the Lock profile.[2]

The layer thickness is expected to grow, and the governing equations (42)-(44) are rewritten in terms of the Blasius similarity variable $\eta = Y/\sqrt{\bar{x}}$. The box scheme allows arbitrary spacing in both $\bar{x}$ and η and is second-order accurate since the discretized equations are applied at the centers of cells formed by the $\bar{x}$-η grid. The nodes were distributed so that the spacing between nodes increases at a fixed rate towards the upper and lower edges of the viscous layer:

$$\eta^j = \pm h_1 (1 - h_2^j)/(1 - h_2) \quad (j = 1, 2, \ldots J^{\pm}) ;$$

here $h_1 = 0.005$ and $h_2 = 1.05$. The range $-21 < \eta < 13$ corresponding to $J^- = 110$ and $J^+ = 100$ was found to be adequate for the inner solution to smoothly reach its asymptotic boundary values. While spectral techniques were used conveniently in the inviscid region, they become inordinately expensive as the resolved spanwise wavenumber is increased beyond 32 (many general matrices of the order of the maximum wavenumber need to be inverted), and instead, second-order, finite-difference, upwind formulae were used in the viscous solution. The symmetry of the external flow is imposed on the viscous solution and, as is well known, the solution on the planes of symmetry, $z = 0, \pi$, can be obtained independently of the solution in the region between these planes. We therefore calculated the solution on the $z = 0$ symmetry

plane and obtained the solution on interior lines by marching from $z = 0$ to $z = \pi$. Since the spanwise velocity W remains positive everywhere in $0 < z < \pi$, this can be carried out without iteration.

The external crossflow and its distortion of the vortex sheet cause the flow to depart from the Lock profile, with the most noticeable changes being the increase in layer thickness on the $z = \pi$ plane and the decrease on the $z = 0$ plane. Figure 8 shows the increasing distortion of the streamwise velocity profiles with increasing downstream distance. Figure 9 shows the corresponding spanwise velocity profiles. Vector plots of the crossflow are shown in figure 10. Note that the transverse velocity is $O(\epsilon R)^{-1/2}$ smaller than the spanwise velocity. The pair of transverse jets (figure 10) at the upper edge of the viscous layer correspond to the reversal in the steepening of the spanwise velocity in figures 4 and 5. This follows from expanding the inviscid solution in a Taylor series and using continuity to obtain

$$\overline{v} = \overline{y}\left(\frac{\partial \overline{v}}{\partial \overline{y}}\right)_{\overline{y}=0} + \cdots = -\overline{y}\left(\frac{\partial \overline{w}}{\partial z}\right)_{\overline{y}=0} + \cdots .$$

4. Concluding Remarks

Plane mixing-layer flows, being inviscidly unstable, have been observed to rapidly break down and roll up into tightly wound spirals. Two-dimensional mixing effectiveness is inadequate for many technological applications, and three-dimensional mechanisms, such as spanwise roll-up, are sought to increase mixing. In this paper, we show that the cumulative action of weak spanwise vorticity in the external free stream can lead to an O(1) distortion of the

mixing region. Since the vorticity, in our analysis, resides in the external flow, it can be maintained over large streamwise distances without undergoing viscous decay. The formation of an inviscid singularity in the solution suggests, by analogy with studies of the similar Kelvin-Helmholtz problem, that spanwise roll-up will ultimately occur in this flow.

Even though the analysis cannot be extended beyond the initial singularity, it can still yield some useful information about mixing by using it to investigate the effect of the initial vorticity distribution on the location of singularity formation. Early formation of the singularity should lead to enhanced overall mixing.

The authors would like to thank Dr. Stephen J. Cowley of the Department of Applied Mathematics and Theoretical Physics, University of Cambridge, for his helpful suggestions about the singularity and Dr. Stewart Leib for providing us with his computer program.

References

1. R. C. Lock, "The Velocity Distribution in the Laminar Boundary Layer Between Parallel Streams," Q. J. Mech. Appl. Math. 4, 42-63 (1951).

2. G. K. Batchelor, An Introduction to Fluid Mechanics, Cambridge University Press, p. 346 (1967).

3. M. E. Goldstein, S. J. Leib, and S. J. Cowley, "Distortion of a Flat-Plate Boundary Layer by Free Stream Vorticity Normal to the Plate," J. Fluid Mech. 237, 231-260 (1992).

4. M. E. Goldstein, and S. J. Leib, "Three Dimensional Boundary Layer Instability and Separation Induced by Small Amplitude Streamwise Vorticity in the Upstream Flow." Submitted to J. Fluid Mech. (1992).

5. D. W. Moore, "The Spontaneous Appearance of a Singularity in the Shape of an Evolving Vortex Sheet," Proc. R. Soc. Lond., A 365, 105-119 (1979).

6. R. Krasny, "A Study of Singlarity Formation in a Vortex Sheet by the Point-Vortex Approximation," J. Fluid Mech., 167, 65-93 (1986).

7. H. B. Keller, and T. Cebeci, "Accurate Numerical Methods for boundary-Layer Flows: II. Two-Dimensional Turbulent Flows," AIAA Journal, Vol. 10, No. 9, 1193-1199 (1972)

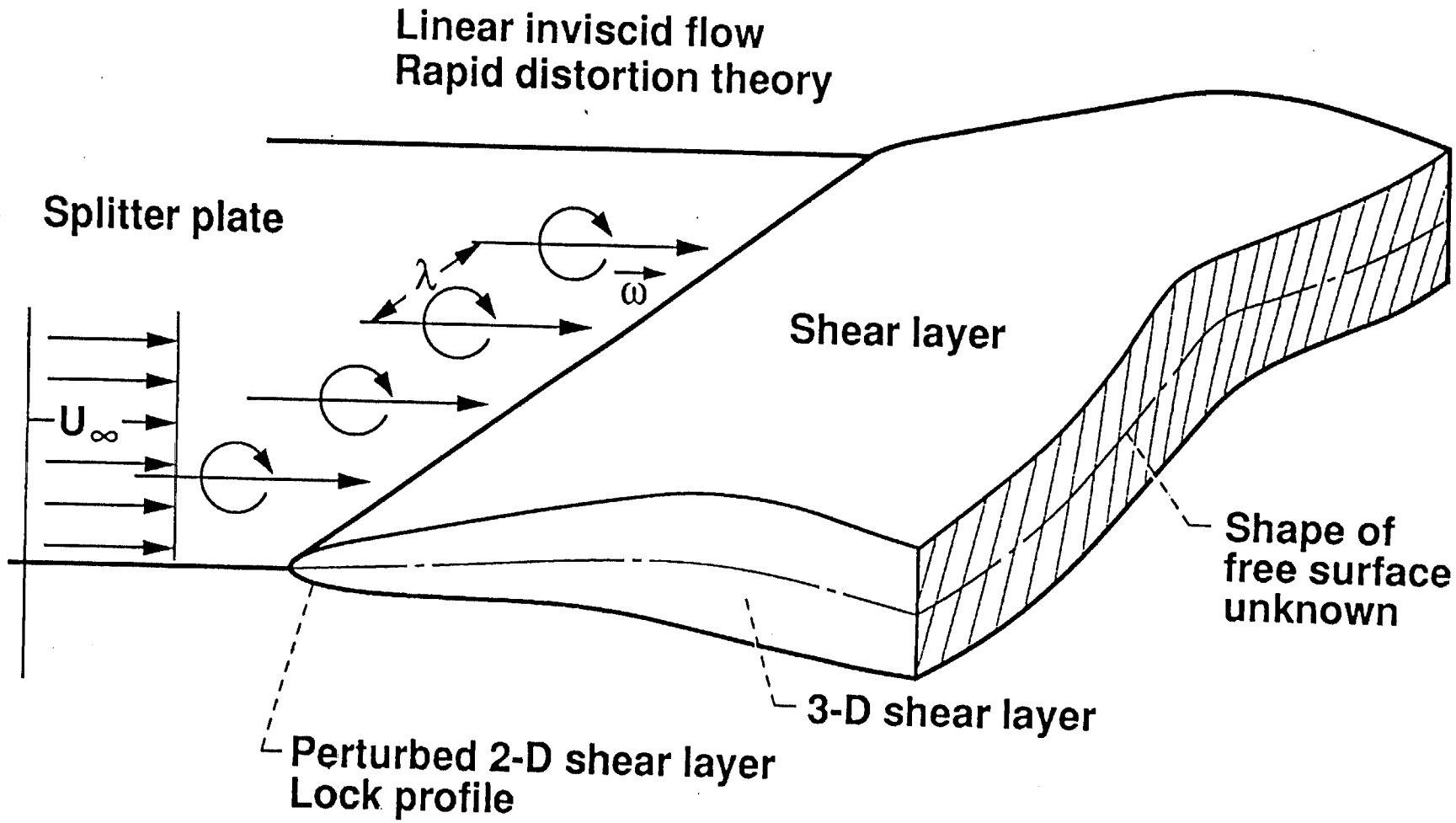

Figure 1 - Flow Configuration

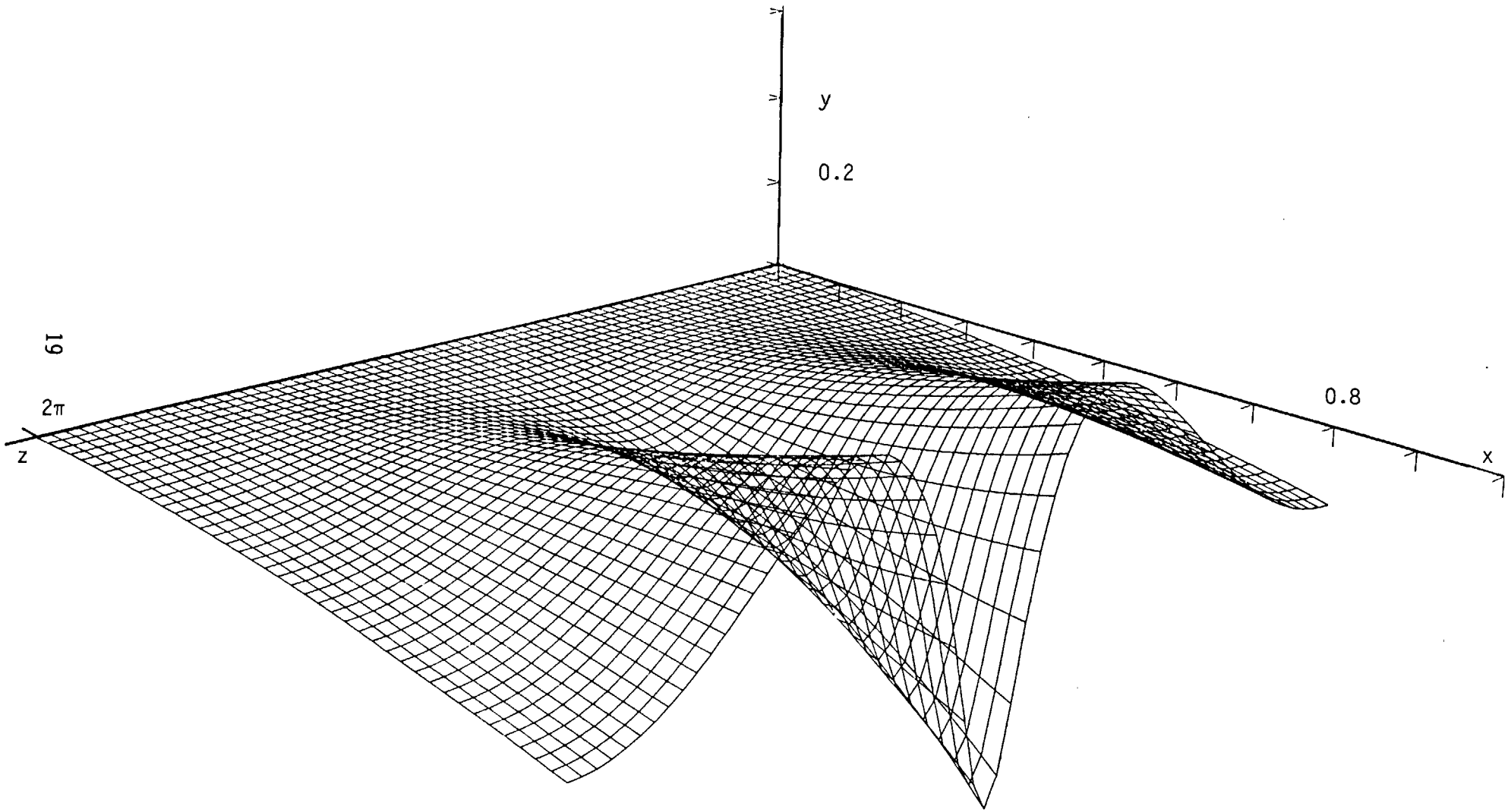

Figure 2

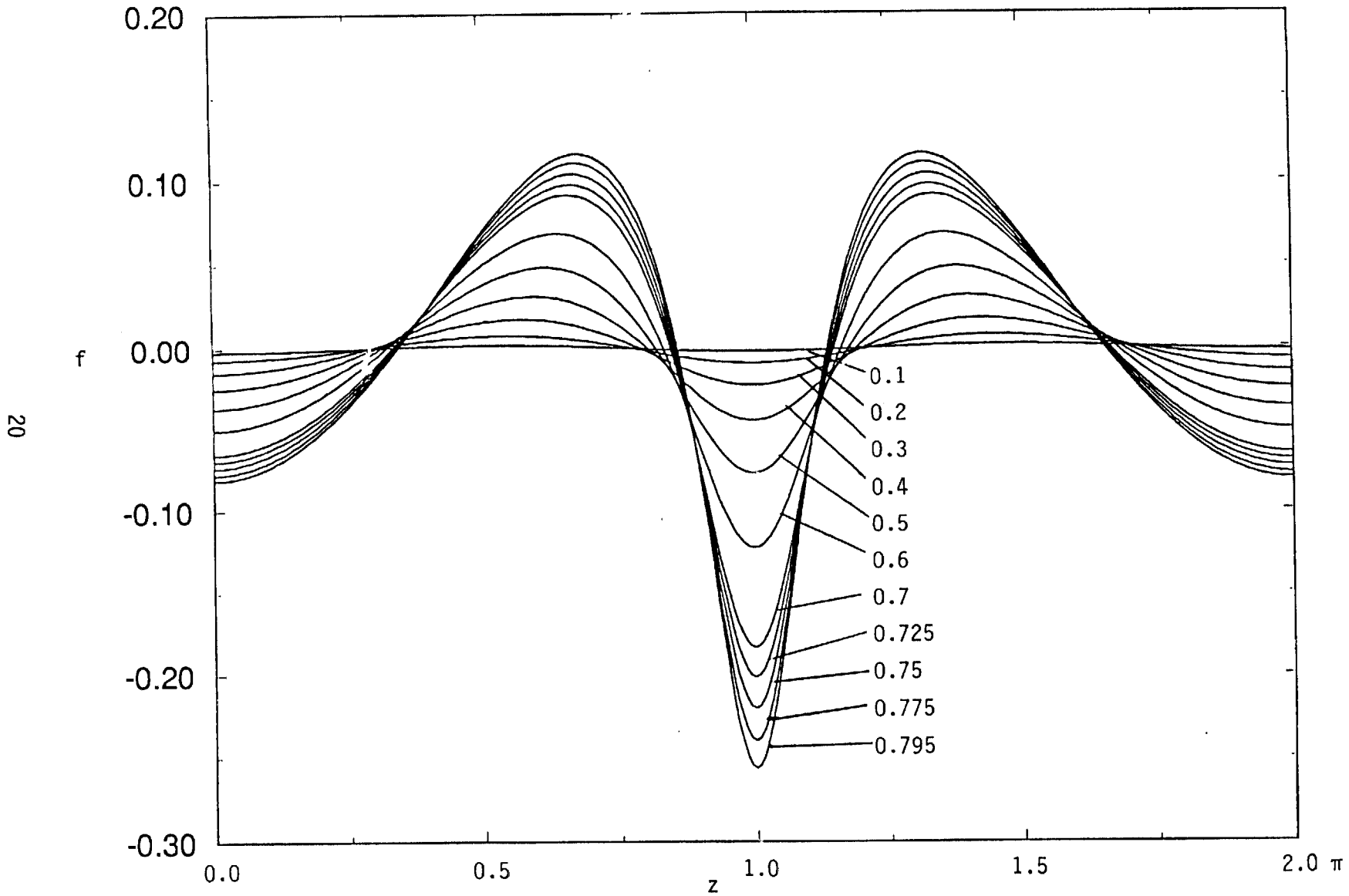
0.20
0.10
0.00
-0.10
-0.20
-0.30
f
0.0
0.5
1.0
1.5
2.0 π
z
0.1
0.2
0.3
0.4
0.5
0.6
0.7
0.725
0.75
0.775
0.795

Figure 3

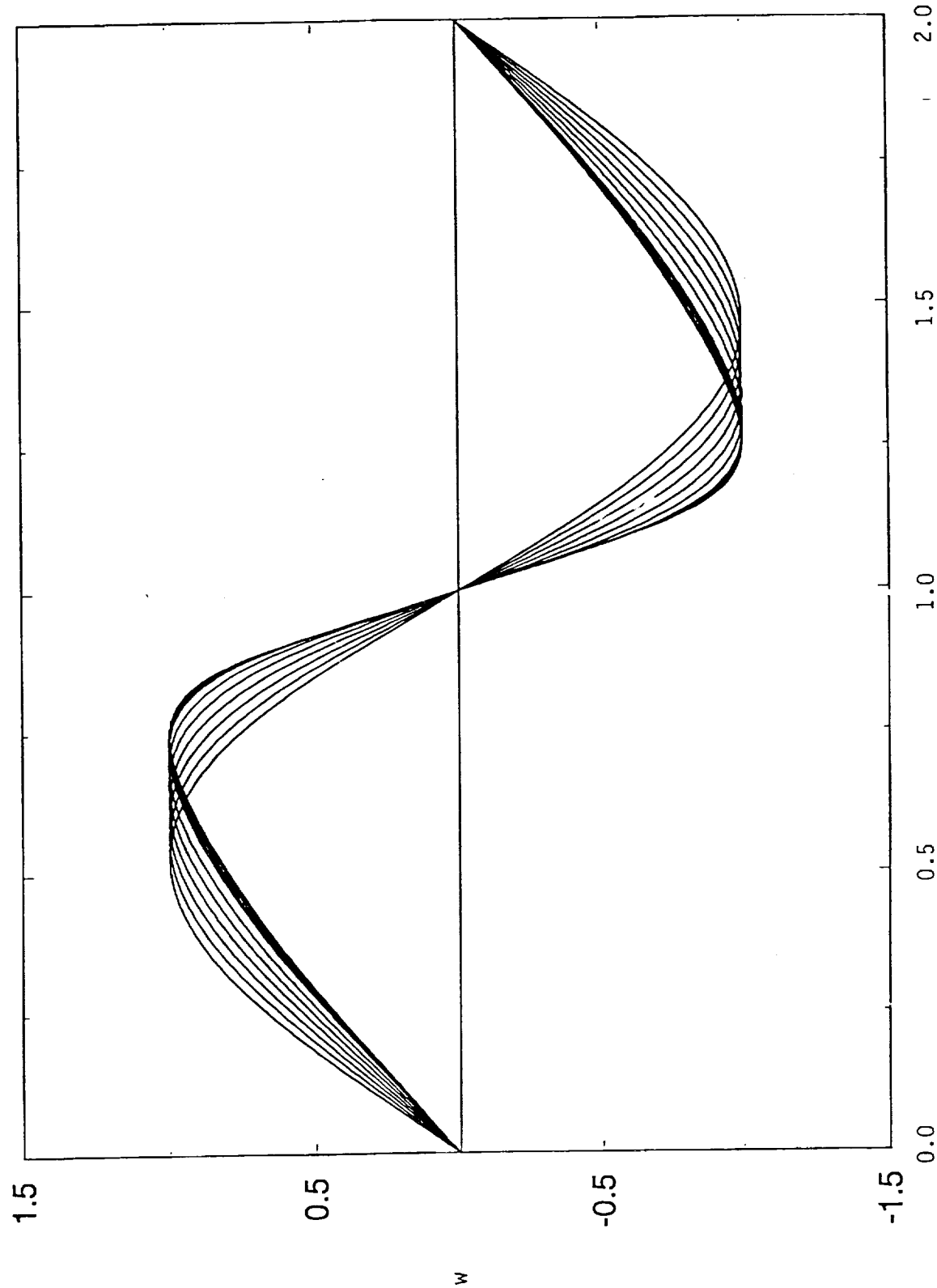

Figure 4

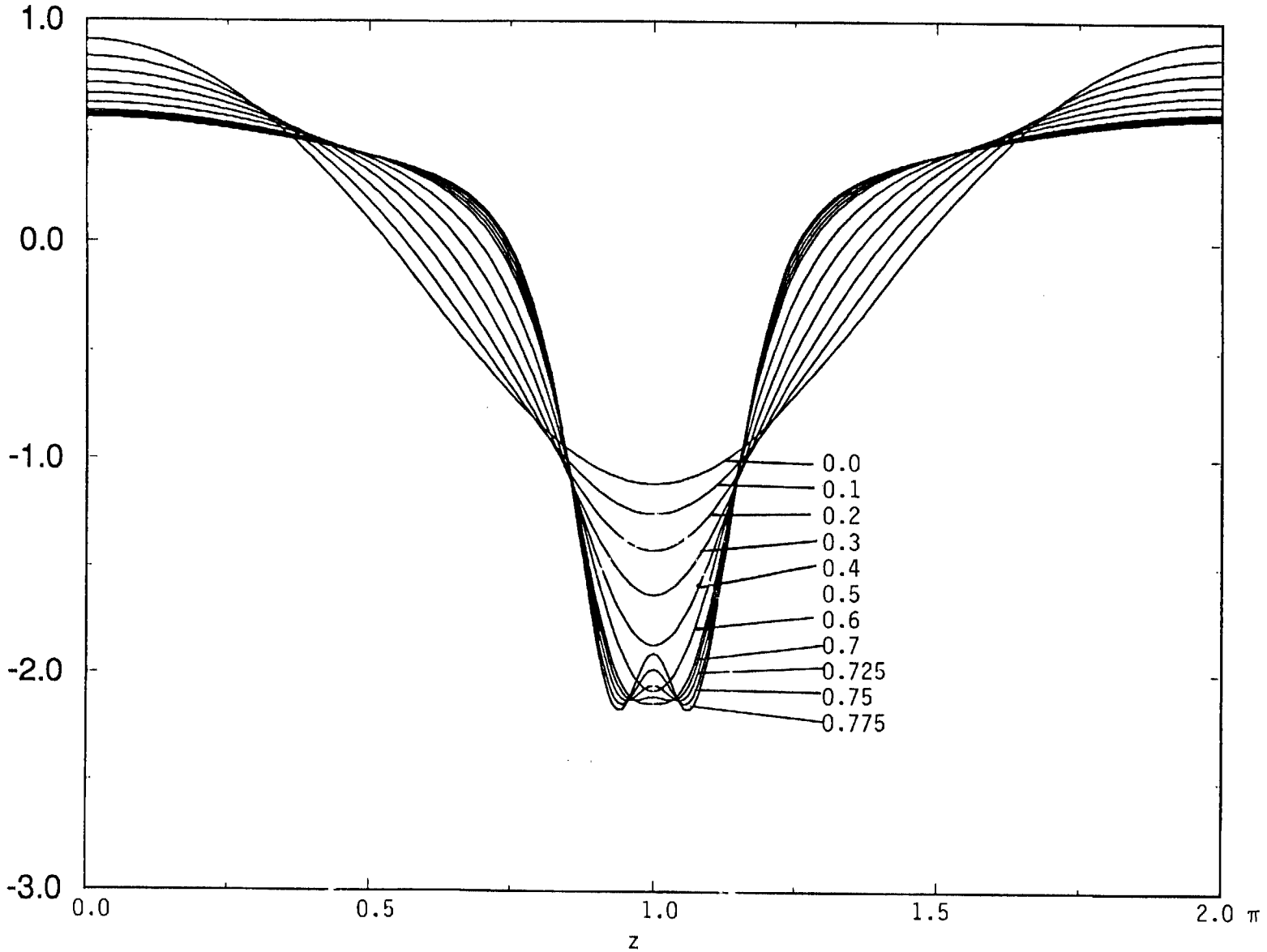
1.0
0.0
-1.0
-2.0
-3.0
0.0
0.5
1.0
1.5
2.0 π
z
∂w/∂z
0.0
0.1
0.2
0.3
0.4
0.5
0.6
0.7
0.725
0.75
0.775

Figure 5

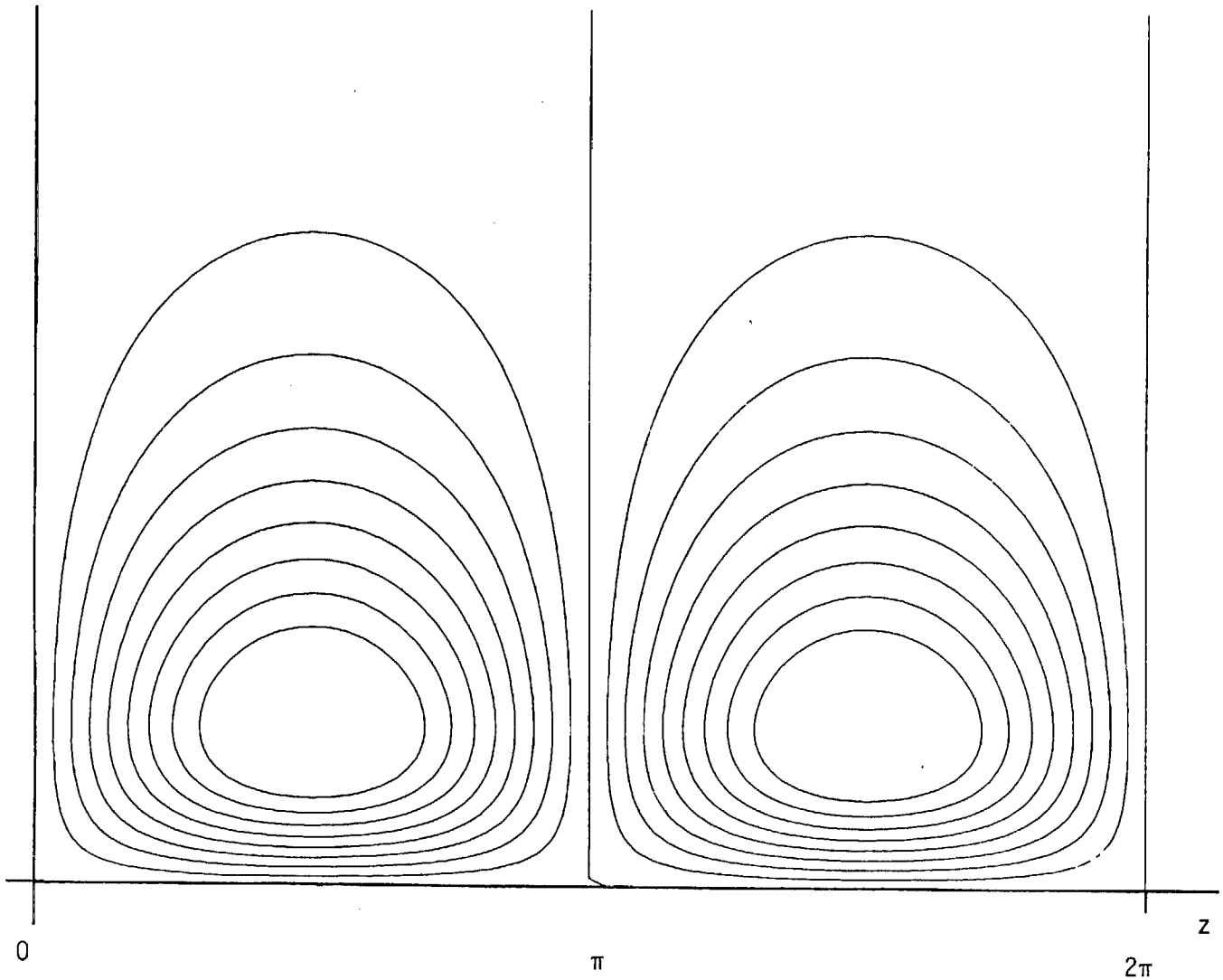

Figure 6 (a) Crossflow Streamfunction $\bar{x} = 0$

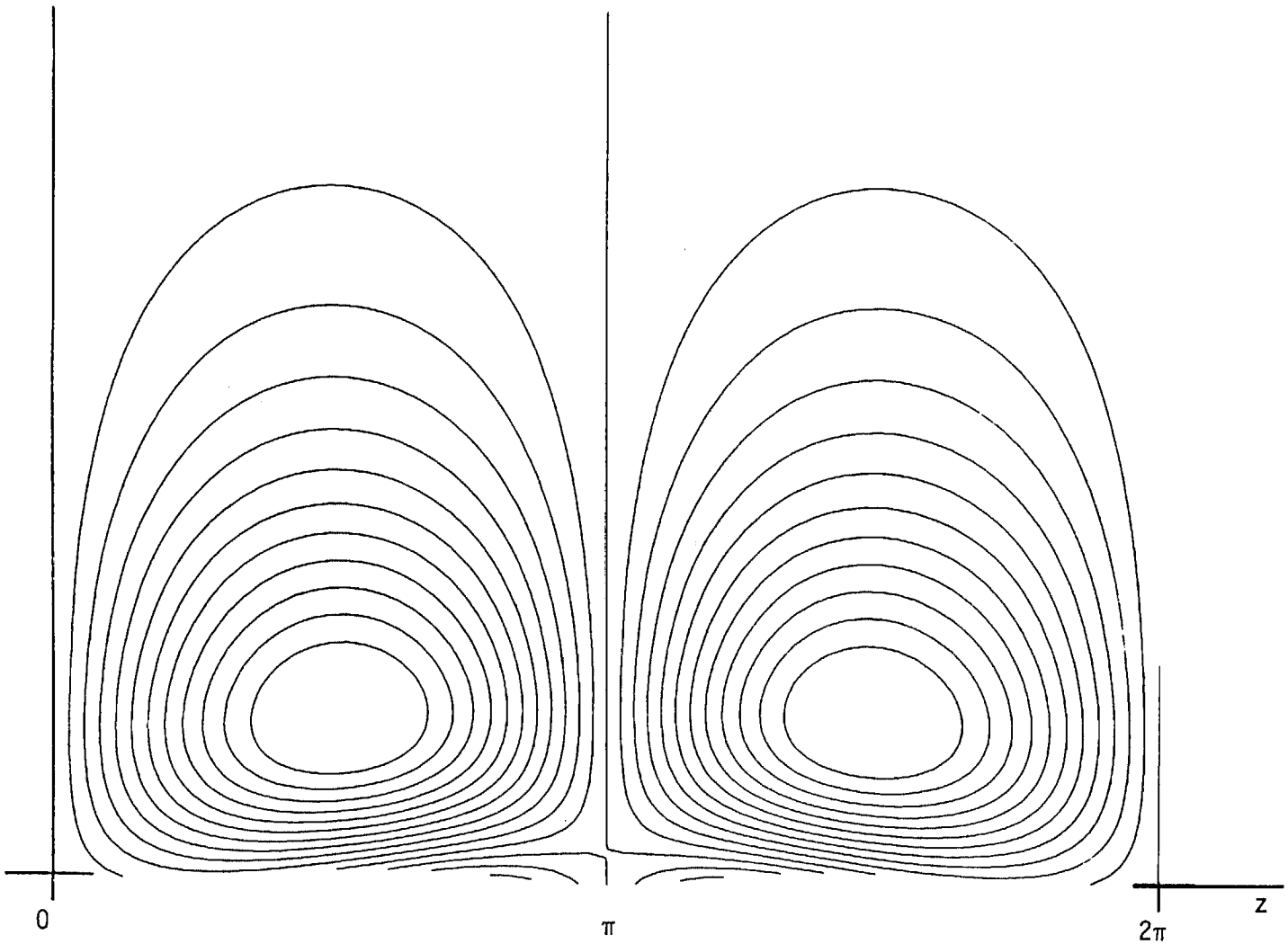

Figure 6 (b) Crossflow Streamfunction $\bar{x} = 0.4$

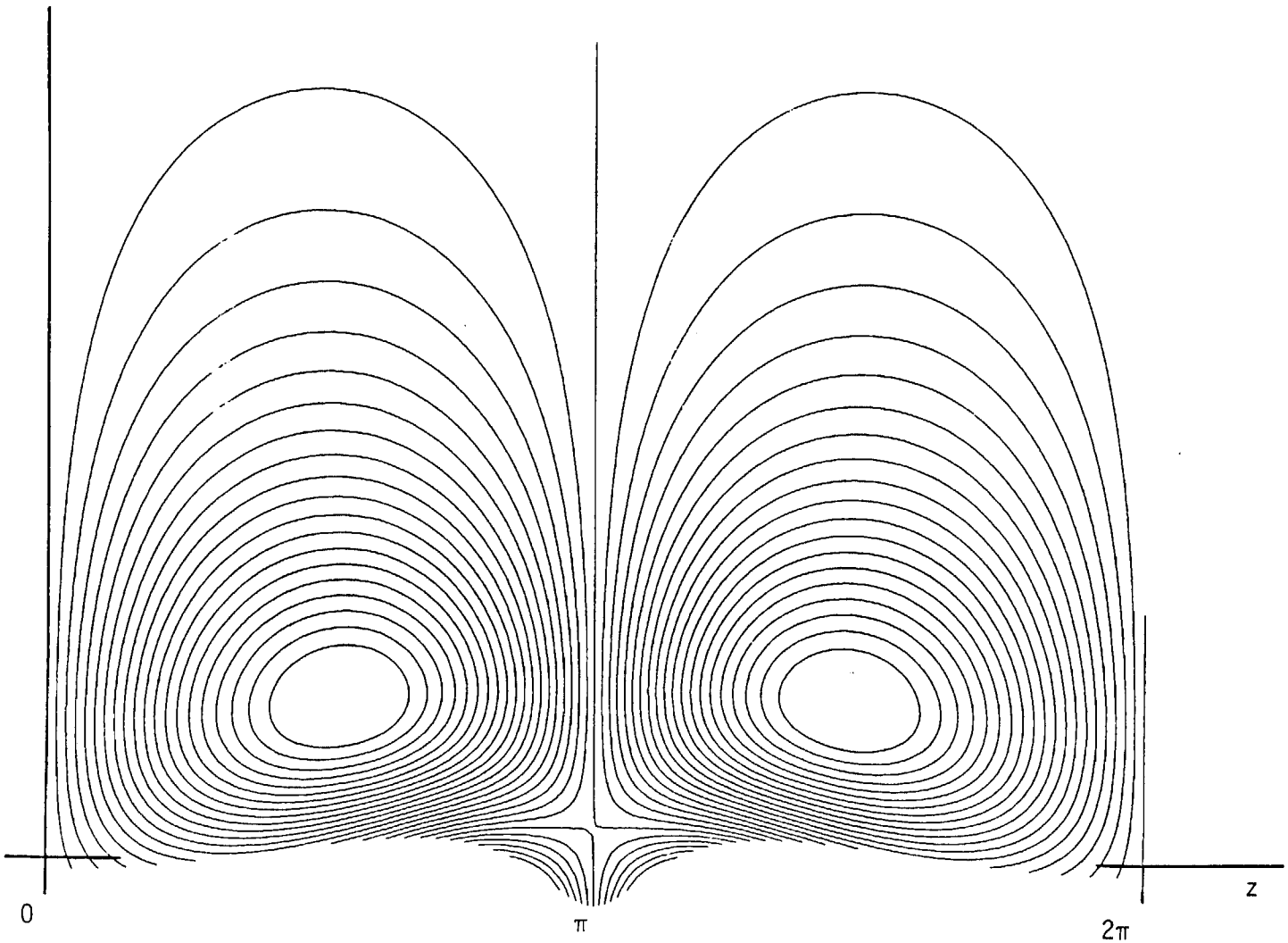

Figure 6 (c) Crossflow Streamfunction $\bar{x} = 0.8$

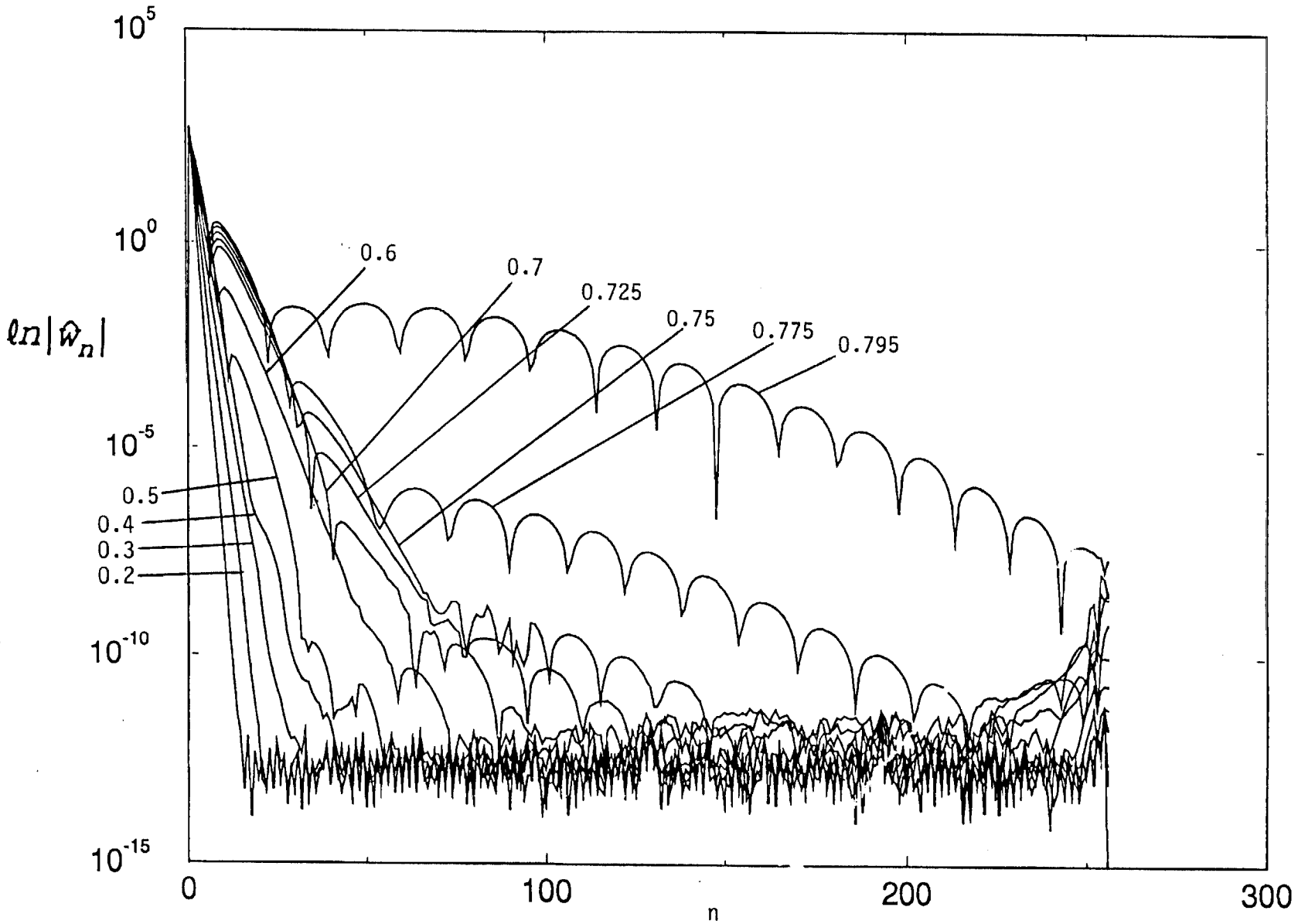
10^5
10^0
10^{-5}
10^{-10}
10^{-15}
$\ln|\hat{w}_n|$
0.6
0.7
0.725
0.75
0.775
0.795
0.5
0.4
0.3
0.2
0
100
200
300
n

Figure 7

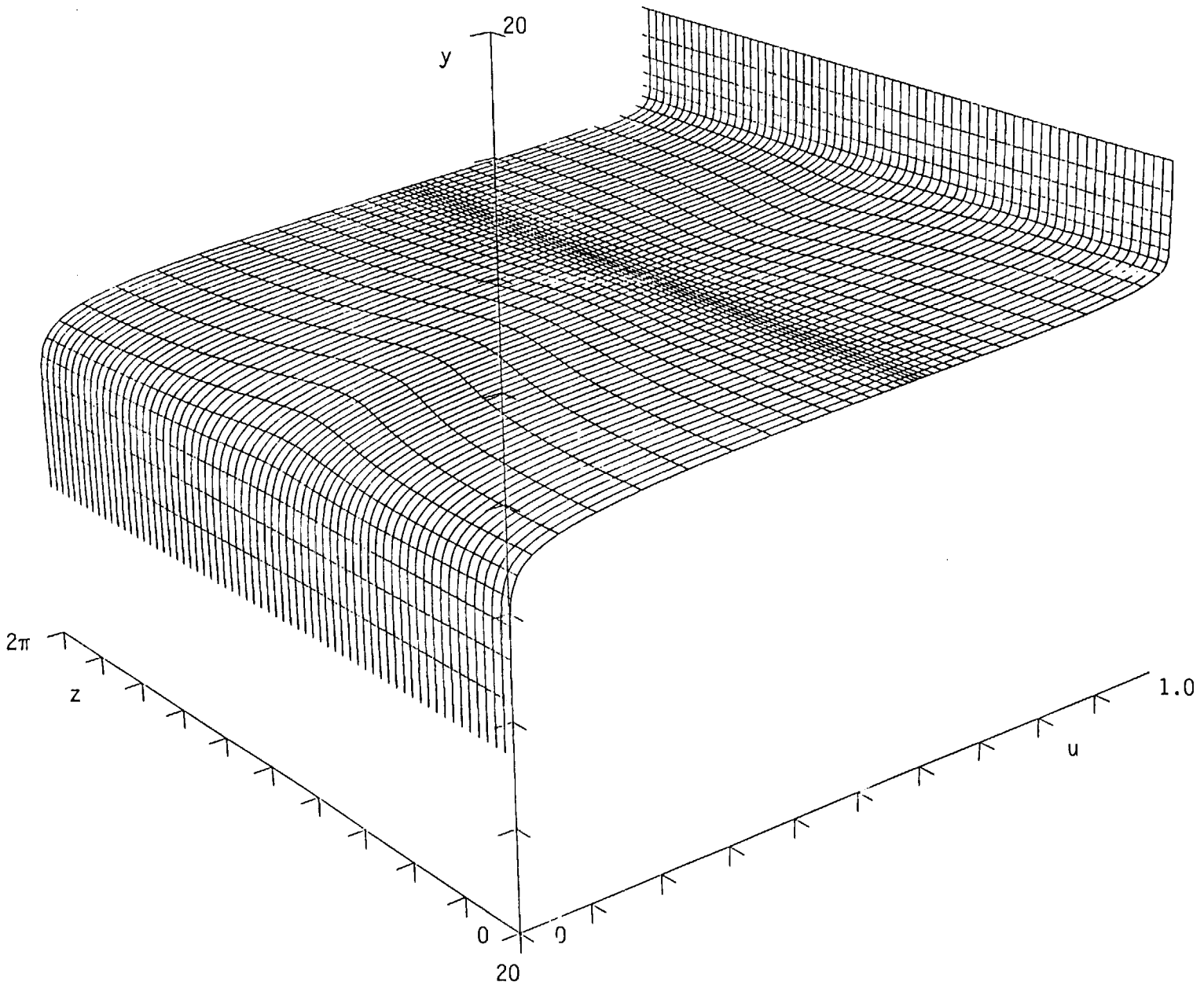

Figure 8 (a) Streamwise Velocity $\bar{x} = 0.3$

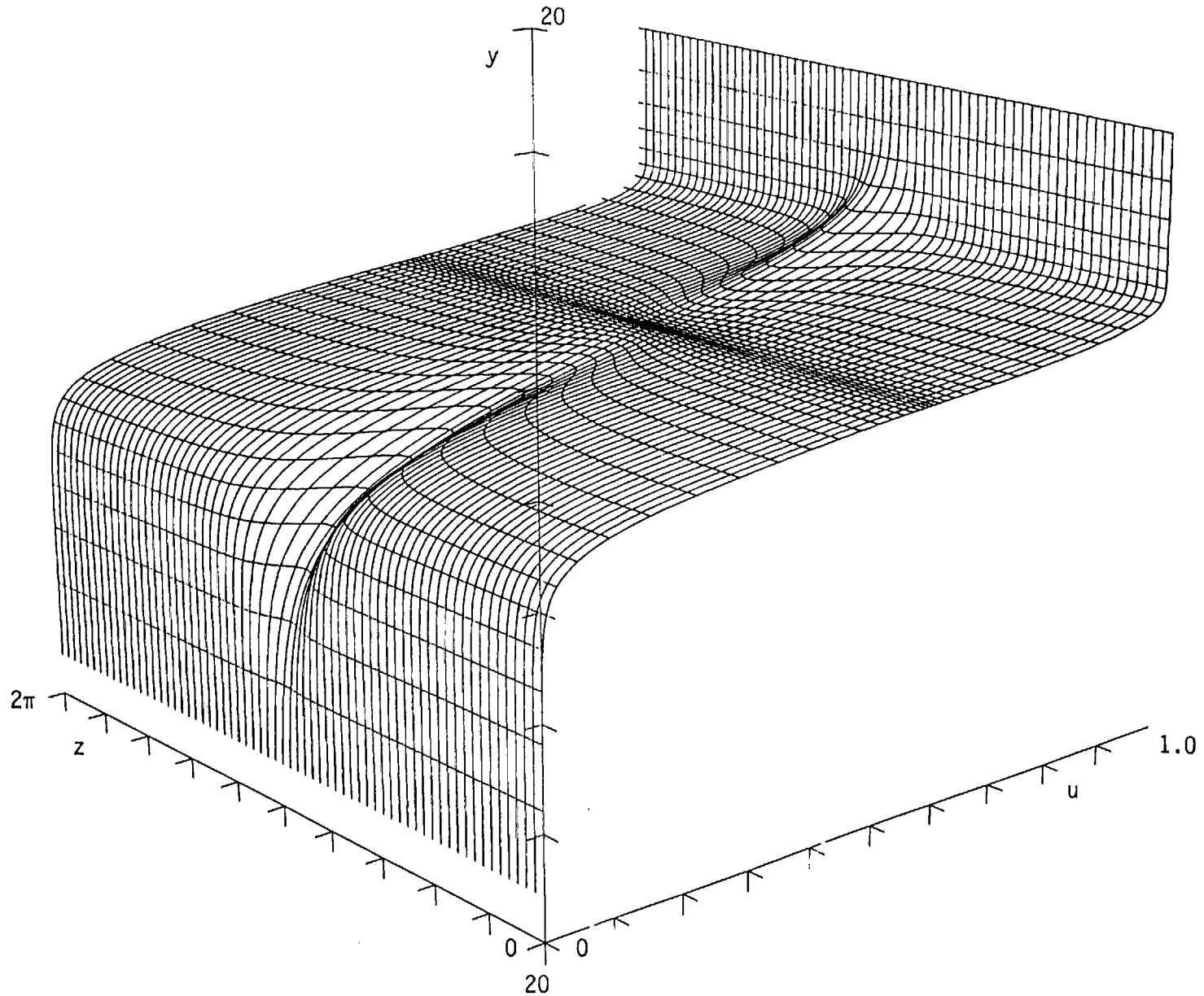

Figure 8 (b) Streamwise Velocity $\bar{x}$ = 0.7

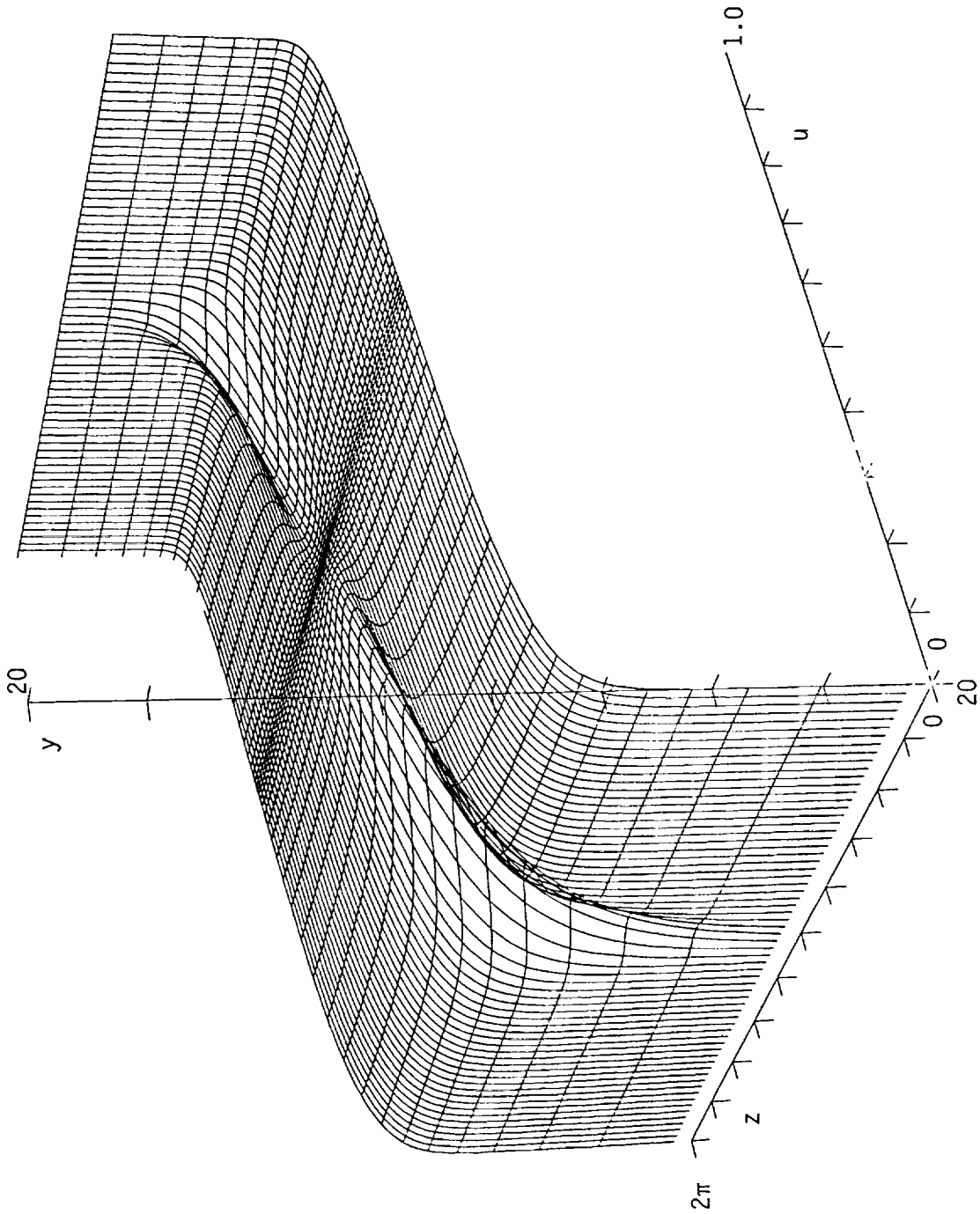

Figure 8 (c) Streamwise Velocity $\bar{x} = 0.795$

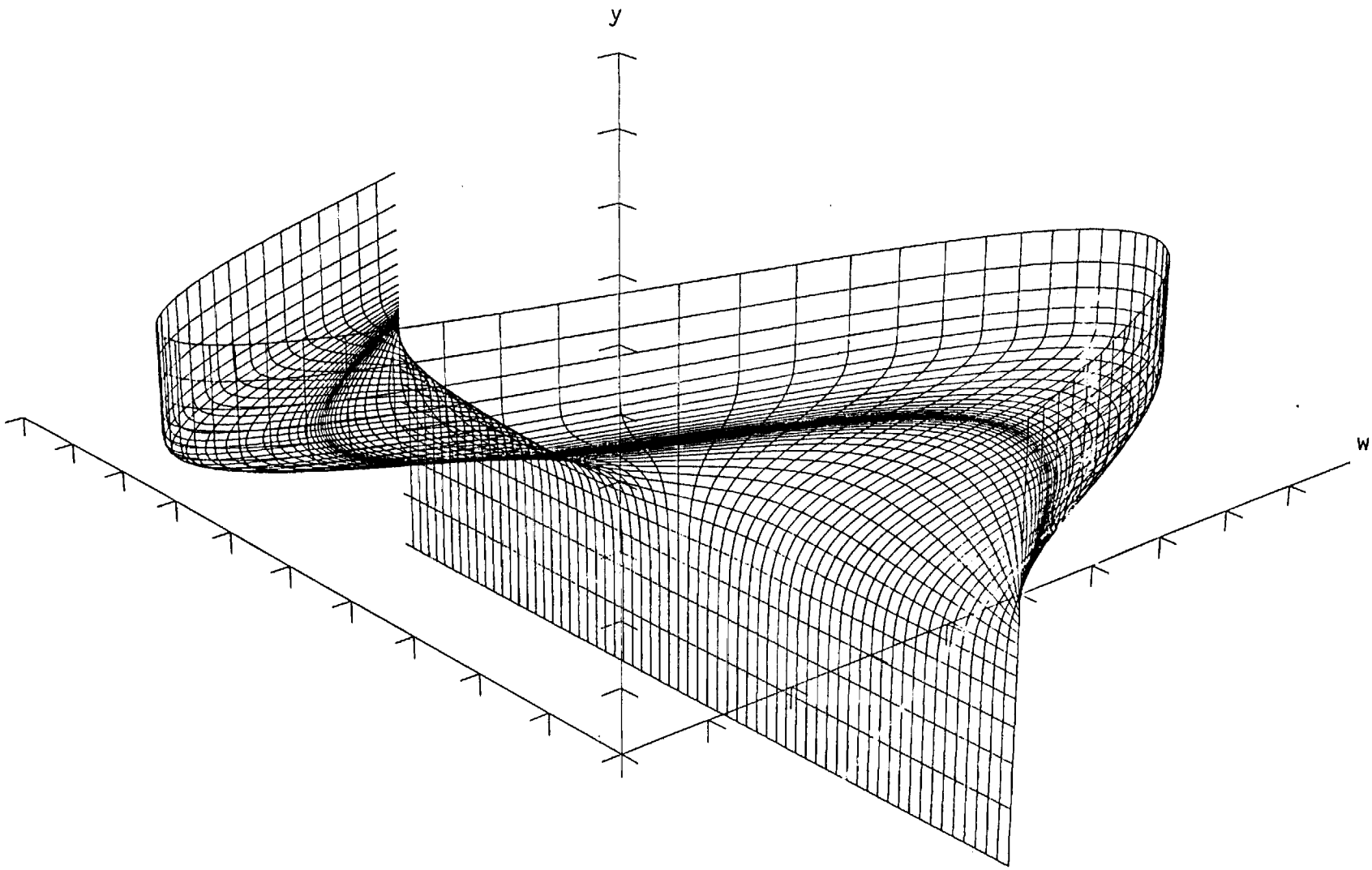

Figure 9 (a) Spanwise Velocity $\overline{x}$ = 0.3

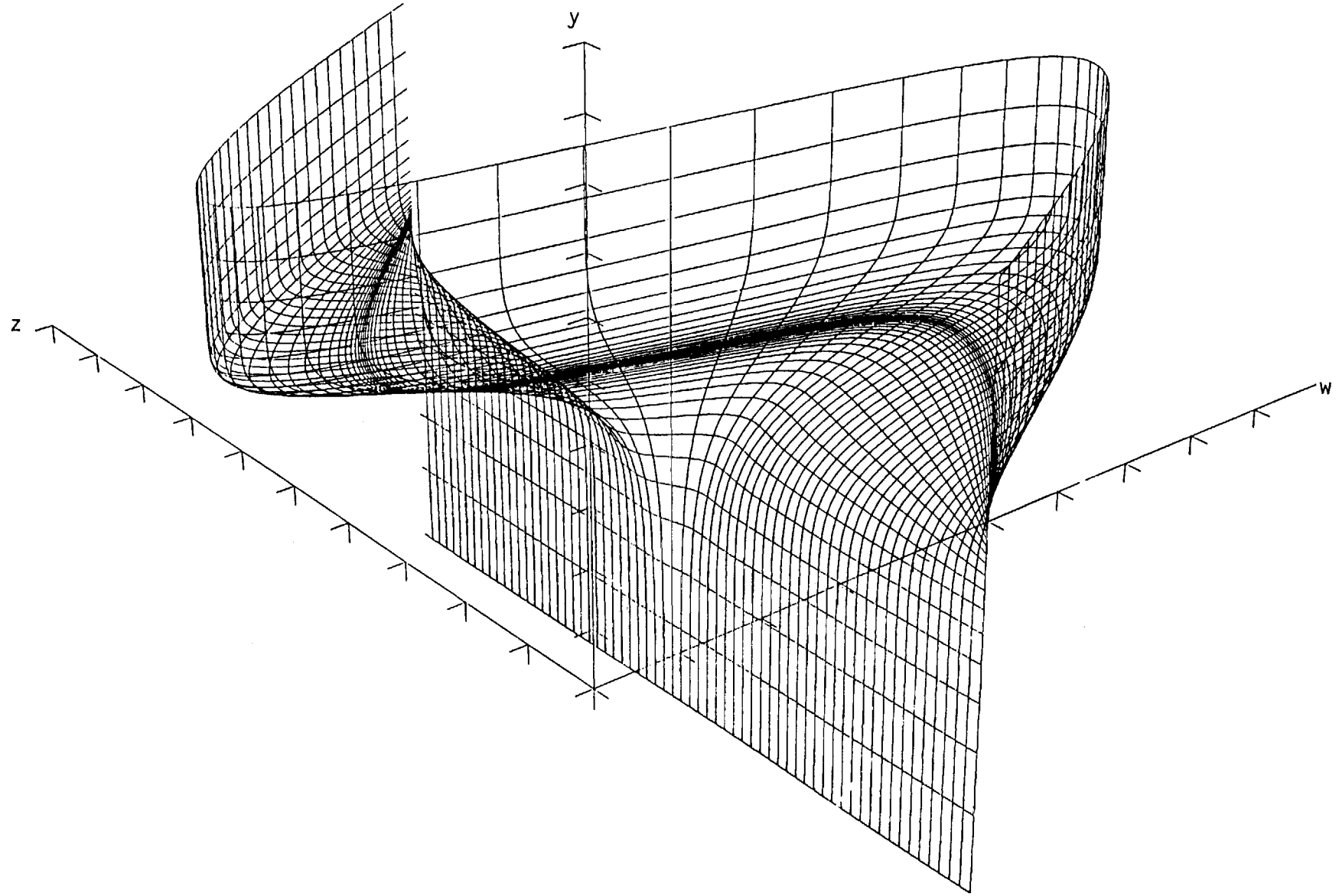

Figure 9 (b) Spanwise Velocity $\bar{x} = 0.7$

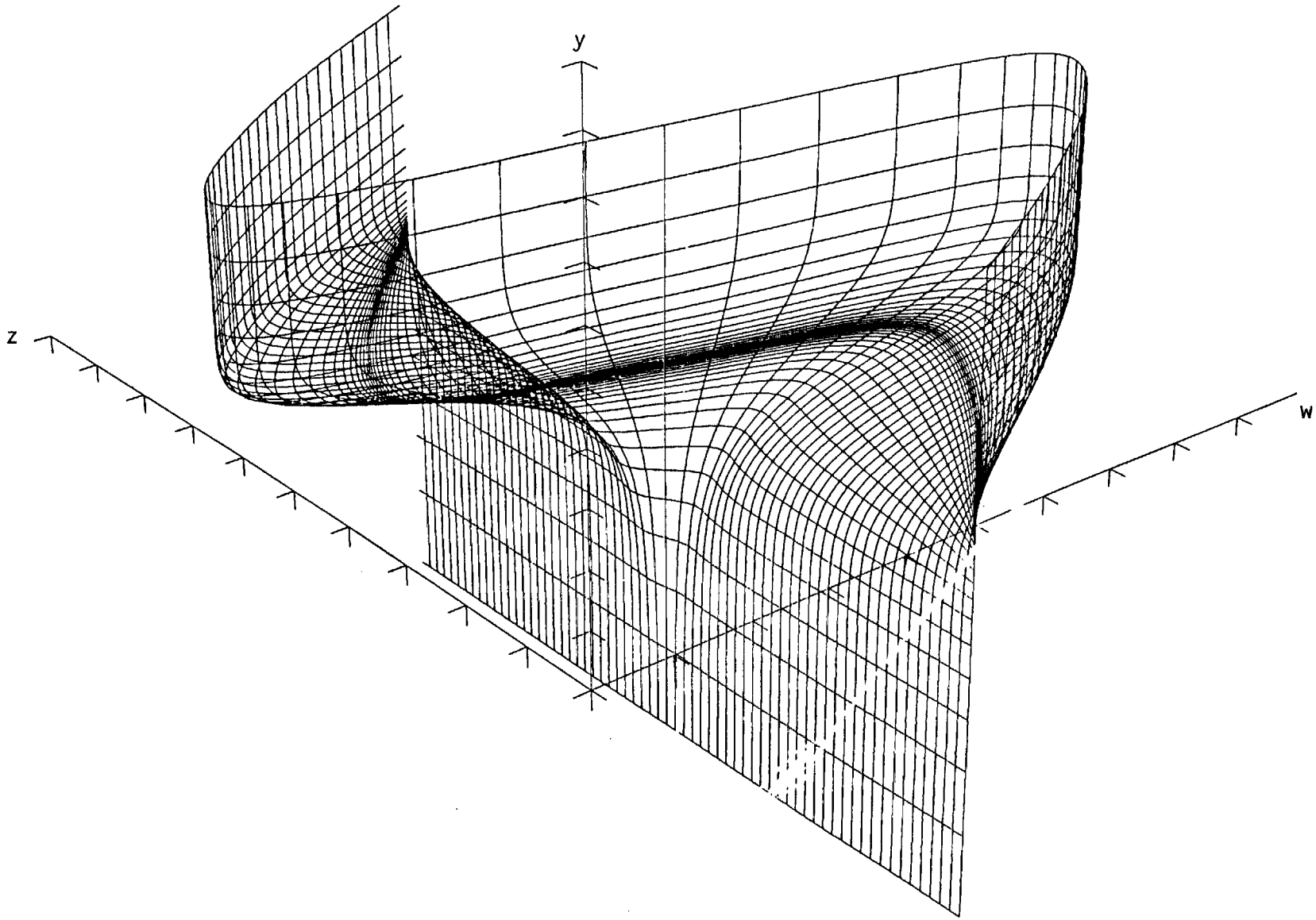

Figure 9 (c) Spanwise Velocity $\bar{x}$ = 0.795

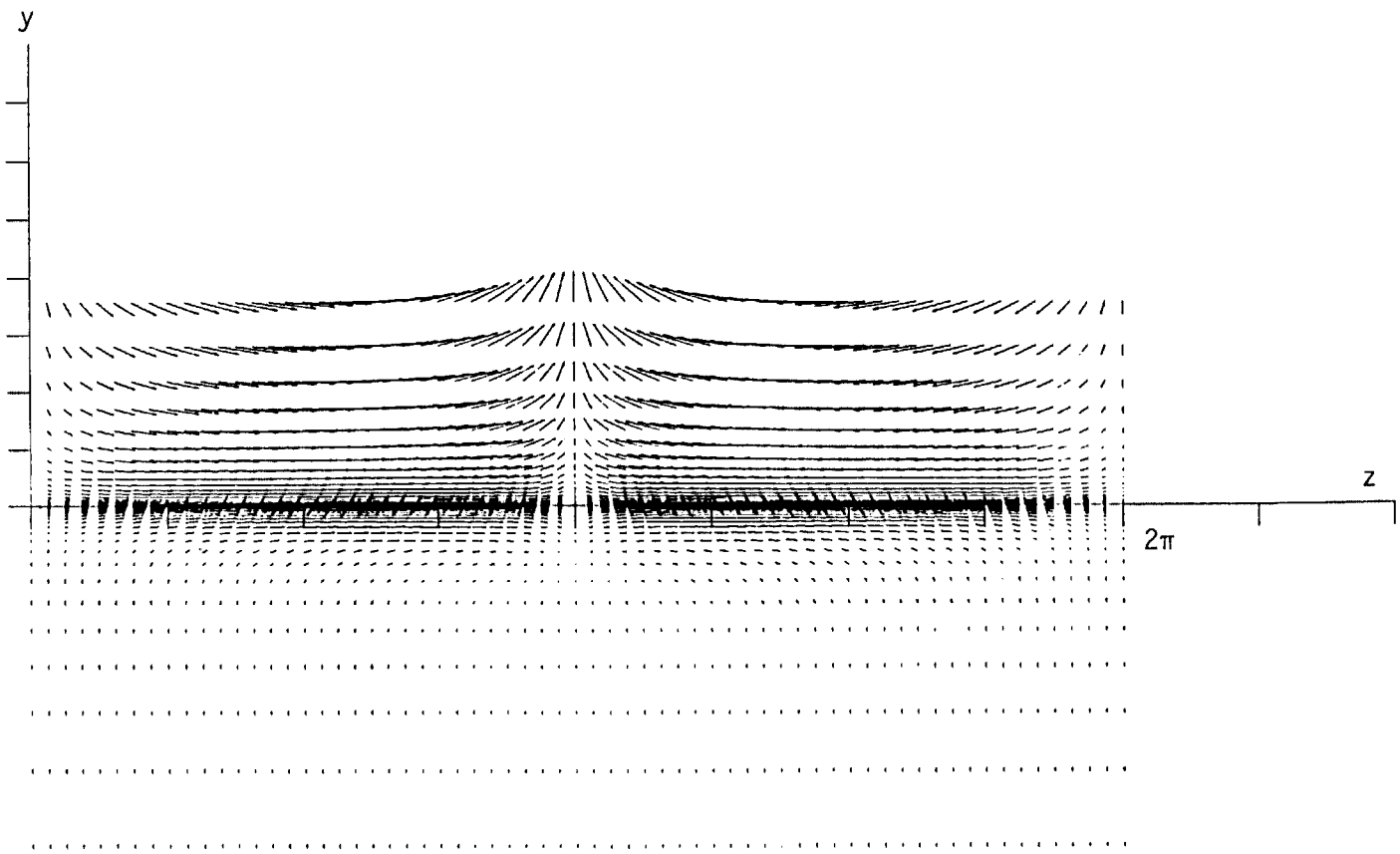

Figure 10 (a) Crossflow Velocity Vector $\overline{x} = 0.3$

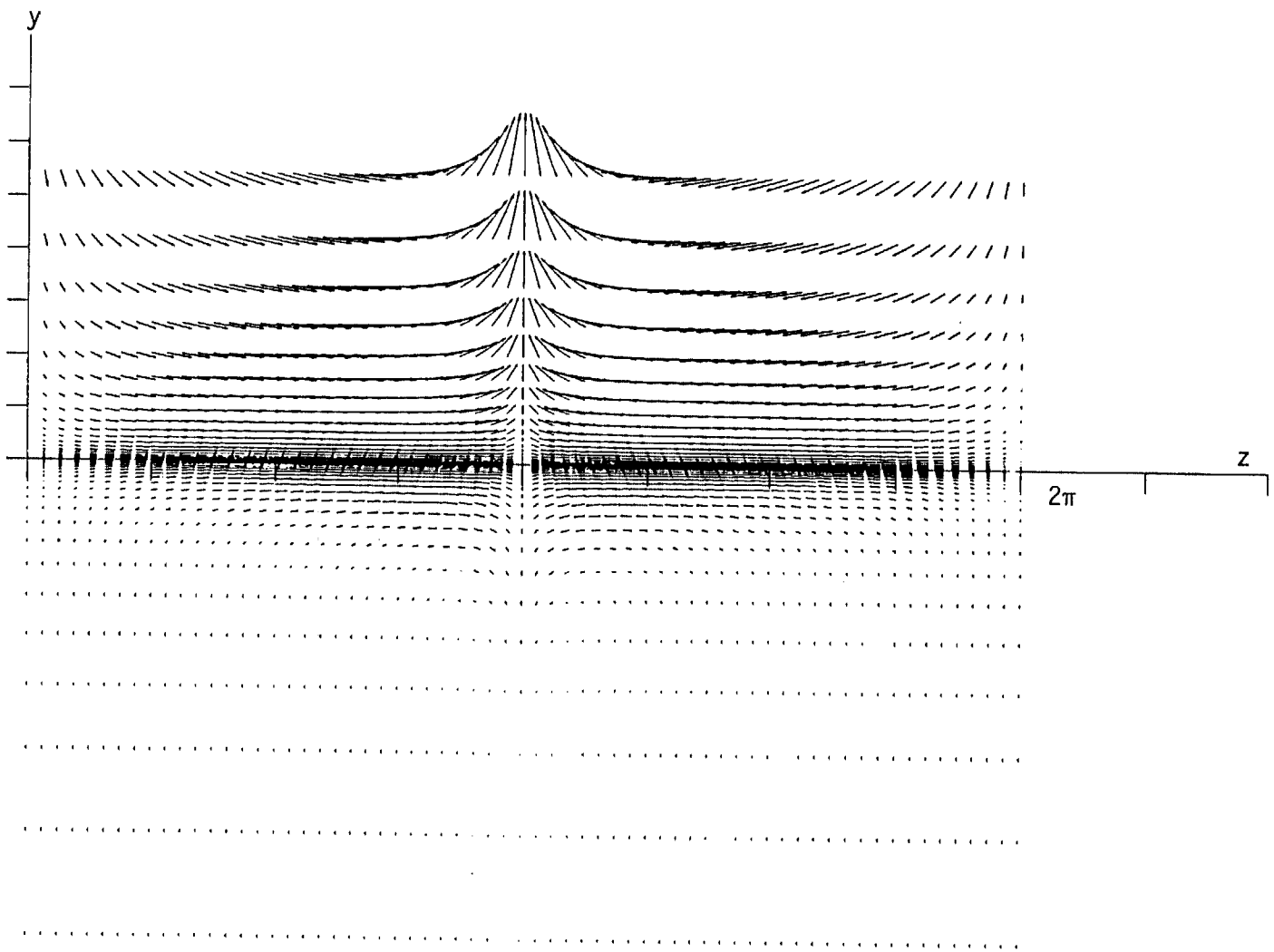

Figure 10 (b) $\bar{x} = 0.7$

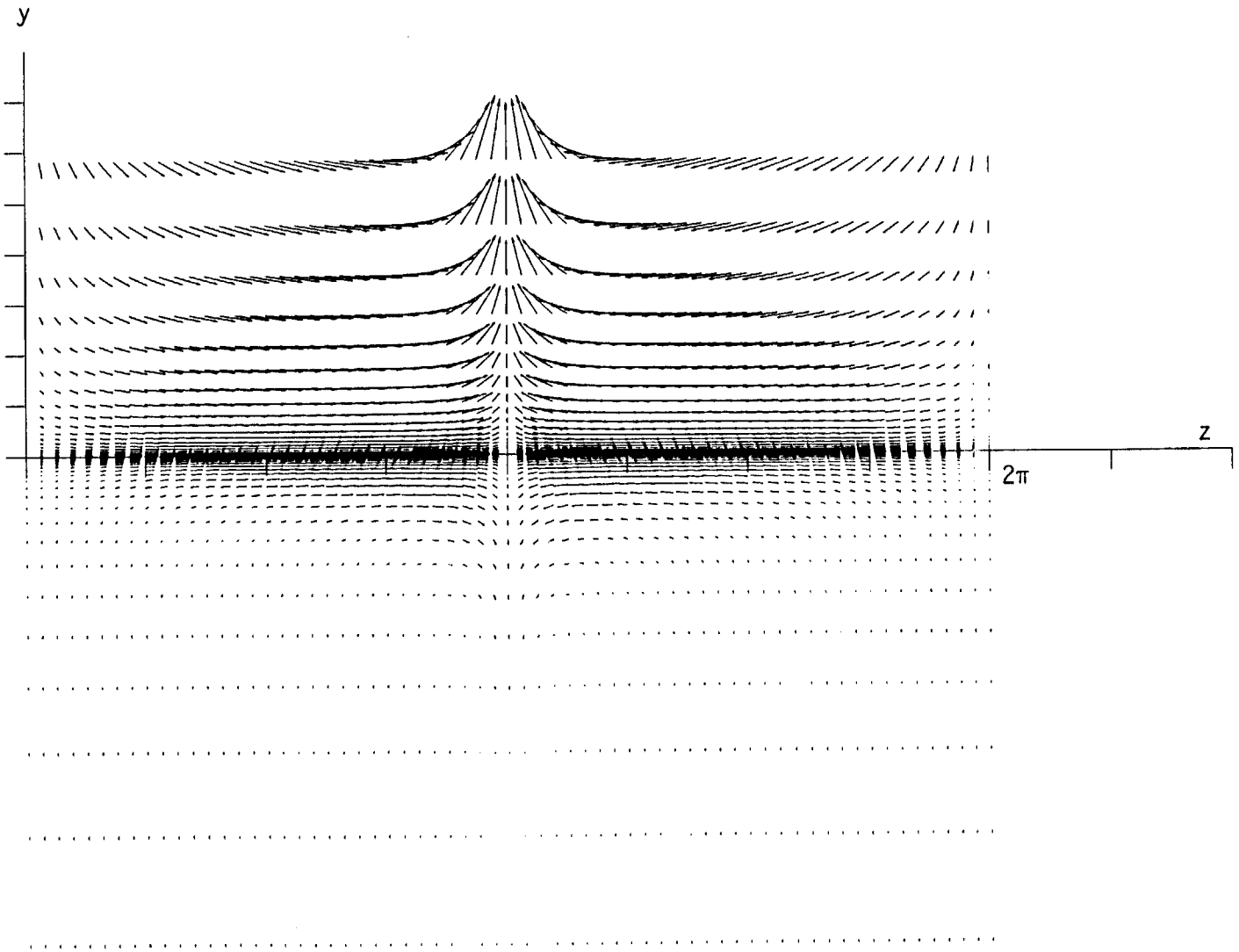

Figure 10 (c) $\bar{x} = 0.795$

REPORT DOCUMENTATION PAGE

Form Approved
OMB No. 0704-0188

1. AGENCY USE ONLY (*Leave blank*)	2. REPORT DATE	3. REPORT TYPE AND DATES COVERED
	March 1993	Technical Memorandum

4. TITLE AND SUBTITLE

The Development of a Mixing Layer Under the Action of Weak Streamwise Vortices

5. FUNDING NUMBERS

WU-505-62-21

6. AUTHOR(S)

Marvin E. Goldstein and Joseph Mathew

7. PERFORMING ORGANIZATION NAME(S) AND ADDRESS(ES)

National Aeronautics and Space Administration
Lewis Research Center
Cleveland, Ohio 44135-3191

8. PERFORMING ORGANIZATION REPORT NUMBER

E-7724

9. SPONSORING/MONITORING AGENCY NAMES(S) AND ADDRESS(ES)

National Aeronautics and Space Administration
Washington, D.C. 20546-0001

10. SPONSORING/MONITORING AGENCY REPORT NUMBER

NASA TM-106089
ICOMP-93-9

11. SUPPLEMENTARY NOTES

Marvin E. Goldstein, NASA Lewis Research Center, Cleveland, Ohio; and Joseph Mathew, Institute for Computational Mechanics in Propulsion, NASA Lewis Research Center, (work funded under NASA Cooperative Agreement NCC3-233). ICOMP Program Director, Louis A. Povinelli, (216) 433-5818.

12a. DISTRIBUTION/AVAILABILITY STATEMENT

Unclassified - Unlimited
Subject Category 34

12b. DISTRIBUTION CODE

13. ABSTRACT ***(Maximum 200 words)***

The action of weak, streamwise vortices on a plane, incompressible, steady mixing layer is examined in the large-Reynolds-number limit: The outer, inviscid region is bounded by a vortex sheet to which the viscous region is confined. It is shown that the local linear analysis becomes invalid at streamwise distances $0(\varepsilon^{-1})$, where $\varepsilon << 1$ is the crossflow amplitude, and a new nonlinear analysis is constructed for this region. Numerical solutions of the nonlinear problem show that the vortex sheet undergoes an 0(1) change in position and that the solution is ultimately terminated by the appearance of a singularity. The corresponding viscous layer shows downstream thickening, but appears to remain well-behaved up to the singular location.

14. SUBJECT TERMS

Vortex sheet; Free shear layer; 3-D Boundary layer

15. NUMBER OF PAGES

36

16. PRICE CODE

A03

17. SECURITY CLASSIFICATION OF REPORT	18. SECURITY CLASSIFICATION OF THIS PAGE	19. SECURITY CLASSIFICATION OF ABSTRACT	20. LIMITATION OF ABSTRACT
Unclassified	Unclassified	Unclassified	